Influence of buoyancy forces on Marangoni flow instabilities in liquid bridges

M. Lappa, R. Savino and R. Monti
Dipartimento di Scienza e Ingegneria dello Spazio "Luigi G. Napolitano", Università degli Studi di Napoli "Federico II", Napoli, Italy

Received January 2000
Revised June 2000
Accepted July 2000

Keywords *Buoyancy, Flow, Fluids, Numerical solutions*

Abstract *The influence of buoyancy forces on oscillatory Marangoni flow in liquid bridges of different aspect ratio is investigated by three-dimensional, time-dependent numerical solutions and by laboratory experiments using a microscale apparatus and a thermographic visualisation system. Liquid bridges heated from above and from below are investigated. The numerical and experimental results show that for each aspect ratio and for both the heating conditions the onset of the Marangoni oscillatory flow is characterized by the appearance of a standing wave regime; after a certain time, a second transition to a travelling wave regime occurs. The three-dimensional flow organization at the onset of instability is different according to whether the bridge is heated from above or from below. When the liquid bridge is heated from below, the critical Marangoni number is larger, the critical wave number (m) is smaller and the standing wave regime is more stable, compared with the case of the bridge heated from above. For the critical azimuthal wave number, two correlation laws are found as a function of the geometrical aspect ratio A.*

1. Introduction

The stability of free convection in non-isothermal liquid bridges with quasi-cylindrical free surfaces has been the subject of intense research. These studies are motivated by the fact that flow instabilities in such configurations may be responsible for the appearance of undesirable striations in crystals grown by the floating zone technique.

There are two types of convection in the floating zone: buoyancy and surface tension-driven convection. On the ground buoyancy convection arises, in the presence of the gravity field, due to density gradients induced by temperature differences applied to the liquid zone. In the microgravity environment provided by drop shaft or drop towers, sounding rockets or space stations, or in microscale experimentation (if the liquid volume is small enough) Marangoni flows, induced by the temperature dependence of the surface tension along the free surface of the zone, prevail over buoyancy convection.

Typically, Marangoni convection is a surface phenomenon and is confined to regions near the free surface, whereas buoyancy drives fluid motion in the bulk of the specimen. Buoyancy forces are in fact "volume" driving actions, whereas Marangoni stresses are "surface" driving actions. It has been demonstrated that

This work is part of the PhD thesis of M. Lappa. The authors would like to thank the Italian Aerospace Research Centre (CIRA) which allowed the numerical calculations on the Silicon Graphics Power Challenge Supercomputer to be made.

Marangoni convection may be subject to instability (Schwabe *et al.*, 1978). This instability may produce undesirable striations in the properties of the crystals produced in microgravity conditions.

In the last two decades a number of experimental works have been performed on the subject by different investigators (Chun and West, 1979; Preisser *et al.*, 1983; Velten *et al.*, 1991; Schwabe *et al.*, 1996; Hirata *et al.*, 1997a, 1997b; Frank and Schwabe, 1998). These studies were carried out on the ground through direct observation of the flow pattern inside the liquid bridge (transparent, high Prandtl number liquids were employed).

Owing to the existence of temperature disturbances on the free surface of the liquid zone, the problem was also investigated in the literature using thermographic techniques. This method was pioneered by Monti *et al.* (1995) and Monti and Fortezza (1986) who were the first to apply this technique to the free surface of a liquid. More recently, Muehlner *et al.* (1997) have investigated the time-dependent features of the instability on the ground using a thermographic system to visualize directly the temperature field. They used an infra-red thermocamera with wavelengths centred at 4.61mm. Since in the wavelength band centred at 4.61mm the substance they used ($Pr = 35$) is partially transparent, these authors observed an average temperature distribution over a depth of about 70 per cent of the radius of the liquid bridge, so that only qualitative results were obtained.

A number of studies have also appeared in which the problem was posed in the framework of linear stability theory to define sufficient conditions for instability in the non-dimensional parameter space (Xu and Davis, 1984; Neitzel *et al.*, 1992; Kuhlmann and Rath, 1993; Wanschua *et al.*, 1995). On the other hand, the development of supercomputers and of efficient numerical methods led the investigators to study the problem through numerical solution of the three-dimensional, non-linear and time-dependent Navier Stokes equations (Rupp *et al.*, 1989; Savino and Monti, 1996; Monti *et al.*, 1997, 1998) which provides information on the features of the supercritical thermo-fluid-dynamic fields also far from the bifurcation point.

It was pointed out (Savino and Monti, 1996; Monti *et al.*, 1997) that for high Prandtl number liquids and unitary aspect ratio, the instability of Marangoni flow is characterized by the appearance of a standing wave instability that, after a certain time, exhibits a second transition to a travelling wave model. This behaviour was confirmed from an experimental point of view by Monti *et al.* (1998) and Shevtsova *et al.* (1998).

In the standing wave regime, maximum and minimum surface temperature disturbances pulsate at fixed azimuthal positions. In the travelling wave regime the disturbances rotate in the azimuthal direction around the axis of the liquid zone.

In the present paper the influence of buoyancy effects on the critical Marangoni number, on the critical frequency, and on the critical azimuthal wave number as well as on the supercritical flow field (pulsating or rotating) is investigated by numerical simulations performed with a 3D numerical code

based on control volume methods and non-uniform grids. Moreover, the numerical simulations are associated with experimental analyses performed using microscale apparatus and a thermographic diagnostic system able to provide direct visualization of the surface temperature spots induced by the Marangoni flow instability on the microzone surface; a thermocamera with wavelengths 8-12mm has in fact been employed that does not make the silicone oil transparent, thus allowing an investigation of the surface behaviour of the temperature field.

The problem related to the influence of buoyancy forces on the features of oscillatory Marangoni convection is particularly important during microscale experimentation on the ground, where gravity and thermocapillary effects are both present.

An excellent analysis of this problem has been given by the experimental work of Velten *et al.* (1991). They studied the influence of gravity on the transition point, frequency and spatial structure of the flow field obtaining a large experimental database. It was observed that the gravity effects can influence both the supercritical spatial organization and the occurrence of the oscillatory regime (pulsating or rotating). This problem has been considered from a numerical point of view partially in the linear stability analyses of Neitzel *et al.* (1992) for Pr = 1, and of Kuhlmann and Rath (1993) for Pr = 4, whose results gave different stability boundaries. More recently, Kuhlmann *et al.* (1996) and Wanschura *et al.* (1997) have considered the combined buoyant-thermocapillary flow for a fixed aspect ratio using linear stability technique.

In the present paper the influence of the gravity field (heating from above or from below) on the critical azimuthal wave number is studied both numerically (numerical solution of the non-linear and time-dependent Navier Stokes equations) and experimentally (microscale apparatus) for different aspect ratios. A "physical explanation" of the influence of gravity effects on the features of Marangoni flow instability (still absent in the literature) is given and a new interpretation of the results obtained by Velten *et al.* (1991) is provided.

2. Physical and mathematical model

Figure 1 shows the geometry of the problem and the boundary conditions. A cylindrical liquid bridge is suspended between two coaxial disks with constant temperatures ($\overline{T} = \overline{T}_0 \pm \Delta T/2$), where $\overline{T}_0$ is the ambient temperature and T the overall temperature difference. The geometrical aspect ratio of the bridge is defined as A = L/D.

The liquid is assumed to be homogeneous and Newtonian, with constant density and transport coefficients. The bridge is bounded by a cylindrical and undeformable liquid-gas interface with a surface tension σ exhibiting a linear decreasing dependence on the temperature: $\sigma = \sigma_o - \sigma_T (\overline{T} - \overline{T}_0)$ where σ_o is the surface tension for $\overline{T} = \overline{T}_0$; σ_T is the negative rate of change of the surface tension with temperature ($\sigma_T = -d\sigma/d\overline{T} > 0$).

The Boussinesq approximation is used to model the buoyancy forces.

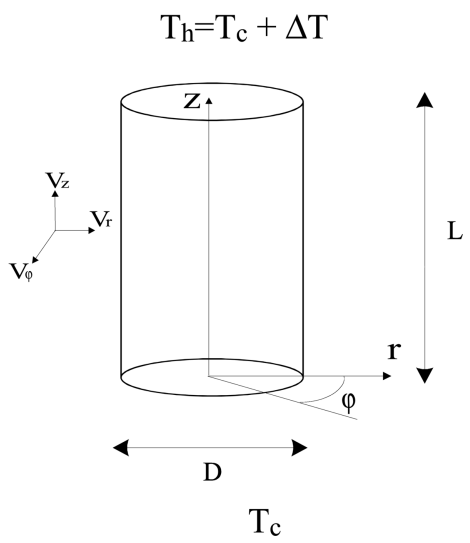

Figure 1.
Sketch of the liquid bridge

With the above assumptions the flow is governed by the continuity, Navier-Stokes and energy equations, that in non-dimensional conservative form read:

$$\underline{\nabla} \cdot \underline{V} = 0 \tag{1a}$$

$$\frac{\partial \underline{V}}{\partial t} = -\underline{\nabla} p - \underline{\nabla} \cdot [\underline{V}\,\underline{V}] + Pr \nabla^2 \underline{V} - Pr\ Ra Ti_{\underline{g}} \tag{1b}$$

$$\frac{\partial T}{\partial t} = -\underline{\nabla} \cdot [\underline{V} T] + \nabla^2 T \tag{1c}$$

where V, p and T are the non-dimensional velocity, pressure and temperature, Pr is the Prandtl number, defined by $Pr = \nu/\alpha$ (ν is the kinematic viscosity and α the thermal diffusivity). The Rayleigh number is defined by $Ra = \frac{g\beta_T \Delta T L^3}{\nu\alpha}$ where β_T is the thermal expansion coefficient. The non-dimensional form results from scaling the lengths by the axial distance between the circular disks (L) and the velocity by the energy diffusion velocity $V_\alpha = \alpha/L$; the scales for time and pressure are, respectively, L^2/α and $\rho\alpha^2/L^2$. The temperature, measured with respect to the initial temperature $\overline{T}_0$, is scaled by (ΔT): $T = (\overline{T} - \overline{T}_0)/(\Delta T)$. The initial conditions are:

$$t = 0 : \underline{V}(z, r, \varphi) = 0, T(z, r, \varphi) = 0 \tag{2}$$

For $t > 0$, the boundary conditions are the non-slip conditions and the condition of prescribed temperatures on the circular disks, the kinematic condition of stream surface (zero normal velocity), the Marangoni conditions (shear stress balance) and the adiabatic condition on the cylindrical interface. Further details on the model are reported in Monti *et al.* (1997, 1998).

3. Numerical solution

3.1 Solution method

The equations (1a-c) and the initial and boundary conditions were solved numerically in cylindrical co-ordinates in primitive variables by a control volume method. The domain was discretized with a non-uniform but structured axisymmetric mesh and the flow field variables defined over a staggered grid.

The finite volume approach relies directly on the application of the integral form of balance laws. Thus the conservation laws have been written for an arbitrary spatial domain Ω bounded by a surface $\partial\Omega$. Forward differences in time were used to discretize the time dependent derivative, obtaining:

$$\underline{V}^{n+1} = \underline{V}^{n} + \Delta t \frac{1}{\Omega}\left[-\int_{\partial\Omega} [\underline{V}\,\underline{V}]\cdot\underline{n}\,dS + \mathrm{Pr}\int_{\partial\Omega}\left[[\underline{\nabla}\,\underline{V}]\cdot\underline{n}\,dS - \mathrm{Pr}\,\mathrm{Ra}\,\underline{i_g}\int_{\Omega} T\,d\Omega\right]^{n} - \Delta t\frac{1}{\Omega}\int_{\Omega}\underline{\nabla}p^{n}\,d\Omega \right. \tag{3a}$$

$$T^{n+1} = T^{n} + \Delta t\frac{1}{\Omega}\left[-\int_{\partial\Omega}[\underline{V}T]\cdot\underline{n}\,dS + \int_{\partial\Omega}[\underline{\nabla}T]\cdot\underline{n}\,dS\right]^{n} \tag{3b}$$

The problem is solved with the well known Marker and Cell method on a parallel supercomputer (Lappa and Savino, 1999).

3.2 Validation of the numerical procedure

The numerical model has been validated by quantitative comparisons with 2D numerical results and with existing three-dimensional linear stability results for Prandtl numbers as close to the one used in the present work as possible.

For two-dimensional computations, Tables Ia and Ib show that values obtained with the present code compare extremely well with those by Kuhlmann and Rath (1993) and Wanschura *et al.* (1995).

Grid size	Minimum stream function
Kuhlmann and Rath (1993)	–4.1
Wanschura *et al.* (1995) 25 × 14	–4.08
Wanschura *et al.* (1995) 50 × 25	–4.10
Present results 20 × 20	–4.03
Present results 24 × 24	–4.075
Present results 30 × 30	–4.094
Present results 40 × 40	–4.10
Present results 50 × 50	–4.103

Table Ia. Minimum stream function of the axisymmetric flow as a function of mesh spacing in the case of uniform grids (A = 0.5, Pr = 10, Ma = 1,000)

A grid refinement study has been also performed to show the numerical convergence of the present algorithm. The computations have been performed for uniform grids Nz × Nr (the first number denotes the number of collocation points in the axial direction, and the second defines the grid size in the radial direction) and for non-uniform grids. For the latter a finer grid has been introduced near the free surface to locally enhance the resolution (Table Ic). The number of points clustered near the free surface are specified using the notation Nz × (Nr_b + Nr_s) (where Nr_s is the number of points stretched near the free surface and Nr_b the points uniformly distributed in the bulk over a radius R_b = 0.7R). The Nr_s points near the free surface are clustered using the stretching function (s) due to Roberts and Eiseman (for further details see Fletcher (1991); for the present computations the stretching control parameters $\mathcal{P}$ = 1 and $\mathcal{Q}$ = 2 have been used). This corresponds to a grid stretching factor δ not constant with a maximum value (δ_{max}) for the layer of points adjacent to the free surface.

To check that the code is able to "capture" the physical instabilities of Marangoni flow, critical Marangoni numbers have been computed and compared with the results of available stability analyses. In particular the case A = 0.5, Pr = 4 (reported in the linear stability analysis of Wanschura *et al.* (1995)) has been considered.

Regarding the definition of the critical conditions for the onset of instability, it is important to clarify the criterion adopted to evaluate the so-called critical Marangoni number.

Table Ib.
Minimum stream function of the axisymmetric flow as a function of mesh spacing in the case of non-uniform grids (A = 0.5, Pr = 10, Ma = 1,000)

Grid size	Minimum stream function
Present results 24 × 24	–4.075
Present results 24 × (20 + 4)	–4.077
Present results 24 × (18 + 6)	–4.085
Present results 24 × (16 + 8)	–4.10
Present results 24 × (14 + 10)	–4.102

Note: The number of points clustered near the free surface (using the stretching function (s) due to Roberts and Eiseman) are specified using the notation Nz × (Nr_b + Nr_s) (where Nr_s is the number of points stretched near the free surface and Nr_b the points uniformly distributed in the bulk over a radius R_b = 0.7R)

Table Ic.
Axial velocity of the axisymmetric flow at z = 0.5 and at different radial positions as a function of grid spacing (A = 0.5, Pr = 10, Ma = 1,000)

Grid size	Vz at r = 0.25	Vz at r = 0.5	Vz at r = 1.0
20 × 20	14.665	16.60	–43.83
24 × 24	14.59	16.624	–43.82
30 × 30	14.504	16.622	–43.80
40 × 40	14.44	16.605	–43.77
24 × (16 + 8)	14.446	16.58	–43.79

The linear stability analyses assume that the critical Marangoni number Ma_c is a threshold value of the Marangoni number at which the growth rate of the disturbances is zero. Typically, in these analyses the critical Marangoni number is computed using an extrapolation of the growth rate to zero. For the present calculations, the critical Marangoni numbers have been defined as those for which the disturbance amplitude tends to vanish (i.e. the non-dimensional azimuth velocity is of the order of 10^{-2}), but is still characterized by a well-defined frequency. These values have been determined using direct 3D simulation rather than extrapolation.

For Pr = 4 and A = 0.5 Wanschura *et al.* (1995) predict m = 2 and $Ma_c \cong 4{,}200$. The present results give $Ma_c \cong 4{,}400$ (5 per cent greater that the linear stability value) and a pulsating regime that develops in a travelling regime after a short transient time. The grid refinement study has been conducted also on the influence of the number of points used in azimuthal direction (Table Id).

Preliminary numerical tests performed with the code on different computers have shown that the time-delay for transition from standing to travelling wave depends on the numerical noise related to the machine used for the simulations. For this reason one should expect differences between the numerical results related to the time-delays presented in the following paragraphs and the times occurring experimentally.

4. Experimental procedure

The experimental facility used to perform the experiments includes a mechanical support system, a temperature control system and a visualisation system.

The support system consists of two cylindrical copper rods, equipped with Peltier elements, which sustain the bridge. The two rods have the same diameter (D = 4 [mm]).

The upper disk can be translated along the vertical axis in order to realize a bridge having the desired aspect ratio. The translation is obtained using a computer-controlled motorized micrometer system.

The temperature control system, which is connected with a tension generator, includes two Peltier elements that establish appropriate temperature on the disks in order to impose the desired temperature differences. The active cooling and heating system is designed in order to reduce the heat transfer

Grid size	f
$24 \times (16 + 8) \times 20$	75.47
$24 \times (16 + 8) \times 25$	78.4
$24 \times (16 + 8) \times 30$	80

Note: The frequency is posed in non-dimensional form using $\cdot D^2/\alpha$ as reference time

Table Id. 3D grid refinement study for A = 0.5, Pr = 4, Ma = 4,800

from the oil to the ambient. The system, based on the Peltier elements, allows the temperature ramps of the two disks to be controlled imposing symmetric temperature profiles with respect to the initial temperature.

Surface temperature distribution is measured by an infra-red thermocamera (it is possible to visualize an extension of the free surface corresponding to an angular range of 160 degrees) capable of acquiring 12fps. The infra-red thermocamera makes it possible to obtain direct visualization of the temperature spots on the surface of the bridge that correspond to the minimum and maximum temperature disturbances.

During an experiment, typically the temperature difference between supports is varied, heating one disk and cooling the other one, with respect to the ambient temperature, with symmetrical temperature ramps and with a very slow ramping rate. When the fully established oscillatory regime is reached, the temperature distribution on the liquid bridge surface is visualized using the infra-red thermocamera.

The thermocamera provides direct visualization of the temperature distribution on the surface of the bridge. The temperature disturbances are computed in a post-analysis phase by subtracting from the surface temperature distribution the time-averaged surface temperature field $T_o(z, \varphi)$ obtained by integrating the experimentally measured surface temperature distribution over the period τ of the oscillations:

$$T_O(z, \varphi) = \frac{1}{\tau}\int_0^{\tau} T(z, \varphi, t)dt = \frac{1}{N}\sum_{i=1}^{N} T_i(z, \varphi) \tag{4}$$

where N is the number of images taken during the period τ.

5. Results and discussion

Parametric numerical analysis has been performed considering several aspect ratios (A = 0.2, A = 0.25, A = 0.3, A = 0.4, A = 0.5). The Prandtl number is Pr = 30 (corresponding to a silicone oil having a kinematic viscosity $\upsilon = 2{\cdot}10^{-6}$ [m^2/s]).

The presence of buoyancy forces (bridge heated from above or from below) has been introduced in order to evaluate the influence of gravity effects on the development and characteristics of instability of Marangoni flow. In the numerical simulations the Rayleigh number corresponding to each case studied has been calculated considering a diameter of 0.4cm for the disks supporting the liquid zone, $g = g_o = 9.81$[m/s^2] and a length $L = D \cdot A$.

Different non-uniform grids have been used to adequately meet the special features of the Marangoni flow in the liquid bridge. For high aspect ratios ($A > 0.3$) the computational points have been distributed almost uniformly in the computational domain, whereas for low aspect ratios ($A < 0.3$) finer grids have been introduced near the free surface to enhance the resolution in the thin Marangoni boundary layer.

For A = 0.5, 24 points have been collocated in the axial direction; this number has been reduced when reducing the length of the liquid bridge (24 for A = 0.5 and 22 for A = 0.2). In radial direction 24 = 16 + 8 points have been used in the case A = 0.5 and 28 = 14 + 14 for A = 0.2 (i.e. the number of points clustered near the free surface has been increased when the aspect ratio is decreased). In particular in azimuthal direction 20 points have been used for $A \geq 0.4$, 30 for $0.2 \leq A \leq 0.3$ (40 for A = 0.2 and heating from above).

5.1 Bridge heated from above

By employing small dimensions of the floating zone it is possible to reduce on the ground the effects associated with buoyancy driven convection in comparison to thermal Marangoni convection.

However, it must be pointed out that even for small heated liquid volumes of the length of some millimetres on earth, the Rayleigh number $Ra = \frac{g\beta_T \Delta T L^3}{\nu\alpha}$ can be of the order of $O(10^3)$ or larger and that the ratio between the Rayleigh number and the Marangoni number $Ma = \frac{\sigma_T \Delta T L}{\rho\nu\alpha}$, which measures the relative importance of buoyancy forces and surface tension imbalance $Ra/Ma = \frac{g\rho\beta_T L^2}{\sigma_T}$, increases quadratically with the characteristic dimension of the liquid zone (L).

In the absence of radial gradients, and if thermocapillary forces are negligible, heating from above should yield a stable linear temperature distribution in the liquid bridge (gravity vector parallel to the density gradient).

If thermocapillary effects are present, buoyancy effects can modify the distribution of the temperature and velocity inside the bridge with respect to the situation of pure Marangoni flow. At the beginning, the case of stable and steady Marangoni flow ($Ma < Ma_c$) will be examined, in order to study the effect of gravity on the laminar Marangoni convection.

The numerical results show that at the centre of the liquid bridge, the velocity in μg is larger than at 1g. The reason for this behaviour is due to the fact that surface tension and buoyancy forces counteract in a liquid bridge heated from above. When gravity changes from μg to 1g, the centre of the vortex appears to move to the interface of the liquid bridge (the radial depth of the vortex cell is decreased (see Figure 2)). The reason is believed to be that the fluid near the cool disk is slowed down by the buoyancy forces; this effect reduces the radial extension of the convection roll.

The influence of the buoyancy effect can also be seen in the temperature field. In zero g conditions a "cold, radially elongated zone" is present near the hot disk, which is created by the return flow that brings cool fluid away from the cold wall along the symmetry axis. The cold liquid is carried towards the hot surface at a rather high position. In normal gravity conditions, since the cold liquid, travelling in the return flow, is slowed down by the buoyancy forces, the temperature of this zone is weakened and consequently the radial temperature gradient near the hot disk is decreased.

Increasing the Marangoni number, the numerical simulations pointed out that, for each case highlighted, the axisymmetric basic state becomes unstable.

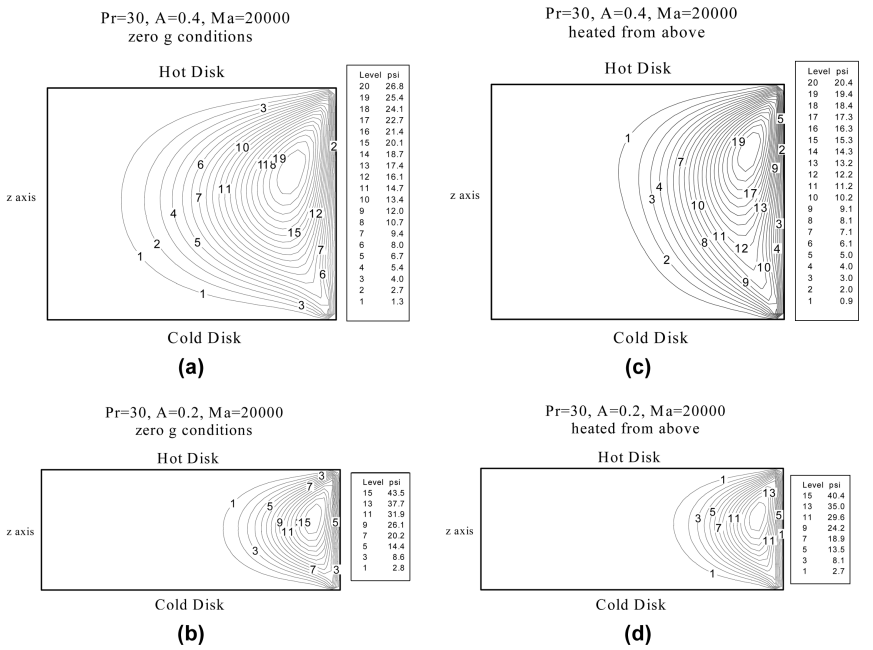

Figure 2.
Streamlines in the generic meridian plane of the liquid bridge: (a,b) zero g condition; (c,d) $g = g_o$; bridge heated from above

When a temperature difference between the supporting disks equal to the critical one is considered, the flow loses its spatial symmetry and a transient unsteady phase develops until a stable supercritical oscillatory three-dimensional state is reached.

The computations indicated that the thermal and flow field organization in the supercritical state may be extremely complex, depending on the geometrical aspect ratio of the liquid bridge (A = L/D).

Similarly to the model of the deformed torus proposed by Preisser *et al.* (1983) the thermo-fluid-dynamic field in the supercritical state, at a fixed time, can be interpreted as the superposition of a sinusoidal azimuthal disturbance to the axisymmetric field, i.e. $F(r, z, \varphi) = F_o(r, z) + \tilde{F}(r, z) \sin(m\varphi)$ where the subscript (o) refers to the axisymmetric field, m is the azimuthal wave number (physically it represents the number of sinusoidal distortions in azimuthal direction). To compare the numerical results with the behaviours predicted by previous stability analyses, the dynamics of the three-dimensional perturbations in the neighbourhood of the bifurcation point were analysed by subtracting the azimuthally averaged field $[F_O(z, r)]$ from the numerically computed three-dimensional time-dependent solution $F(z, r, \varphi, t)$ (average flow + perturbation).

The results, summarized in Table II, show a functional dependence of the azimuthal wave number of the critical mode (m) on the aspect ratio of the liquid bridge. The onset wave numbers are strictly ordered with respect to A. The critical number is m = 2 for A close to 0.5, whereas higher values have been found for lower aspect ratios. Different values of m were obtained in well

defined ranges of the aspect ratio. For instance, Table II shows: m = 2 for $0.3 < A \leq 0.5$, m = 3 for $0.25 \leq A \leq 0.3$ and m = 4 for A = 0.2 (very short liquid bridge).

For m = 2 ($0.3 < A \leq 0.5$), in the generic cross-section orthogonal to the liquid bridge axis (z = 0.5) there are four azimuthal convective cells (Figure 3a) and four thermal spots (two hot and two cold) on the liquid bridge surface. For m = 3 ($0.25 \leq A \leq 0.3$) and m = 4 (A = 0.2) the vortex cells and the surface spots are six and eight respectively (Figure 3b and 3c).

The azimuthal organization of the flow field is characterized by an increasing number of convective cells when the aspect ratio is reduced. Since the azimuthal wave number is related to the aspect ratio, the flow structure of the supercritical state is related directly to the value of m.

Table III shows the numerical and experimental results related to values of the Marangoni number corresponding to typical supercritical conditions ($Ma \cong 1.5\, Ma_c$).

The dependence law between the critical azimuthal wave number and the geometrical aspect ratio provided by the numerical results for heating from above has been confirmed by the experimental results obtained using the microscale apparatus.

In these experiments the value of the critical azimuthal wave number has been determined by observing the surface of the liquid bridge using a thermocamera. The thermocamera gives the number of the spots on an extension of the free surface of the bridge corresponding to 160 degrees. This number represents the critical azimuthal wave number. In fact, on the entire angular extension of the bridge free surface (360 degrees) there are 2m spots (m hot and m cold): if the thermocamera provides the number of the spots on 160 degrees, this number is m.

For A = 0.4 there are two thermal spots on the bridge surface and hence m is 2 (Figure 4a-h shows the surface disturbance temperature distribution determined numerically and experimentally respectively; in this Figure the period τ has been divided into four parts and the temperature field is shown in Figure 4a,b,c,d corresponding to t = 0, $\tau/4$, $\tau/2$, $3\tau/4$); for A = 0.25 there are three thermal spots on the bridge surface and hence m is 3 (Figure 5a-d shows the surface disturbance temperature distribution determined numerically and experimentally respectively; in these Figures the period τ has been divided into two parts and the temperature field is shown in Figure 5a,b corresponding to

A	Ra	Ma_c	m	$f \cdot 10^{-2}$	$Vp \cdot 10^{-2}$	m (zero g)	$f \cdot 10^{-2}$ (zero g)
0.2	$-2.9\ 10^3$	$2.5\ 10^4$	4	11.82	9.27	4	11.36
0.25	$-4.42\ 10^3$	$2.45\ 10^4$	3	7.79	8.16	3	7.38
0.3	$-6.17\ 10^3$	$2.4\ 10^4$	3	5.91	6.18	2	5.17
0.4	$-1.09\ 10^4$	$2.35\ 10^4$	2	3.55	5.57	2	3.08
0.5	$-1.62\ 10^4$	$2.25\ 10^4$	2	2.72	4.26	2	2.77

Table II. Influence of the aspect ratio on the critical parameters (numerical results, bridge heated from above)

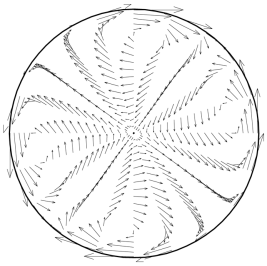

(a)

Velocity field in the section z=0.5 for A=0.5 (bridge heated from above, m=2, Ma= 3.5 10^4)

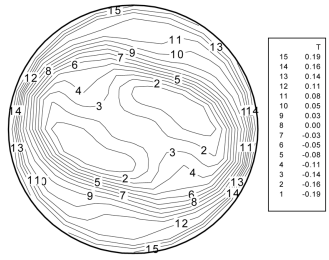

(d)

Temperature field in the section z=0.75 for A=0.5 (bridge heated from above, m=2, Ma= 3.5 10^4)

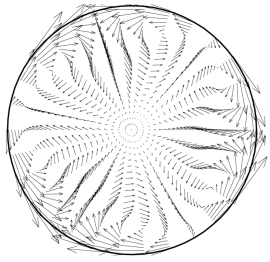

(b)

Velocity field in the section z=0.5 for A=0.25 (bridge heated from above, m=3, Ma= 3.75 10^4)

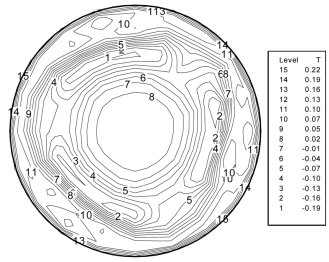

(e)

Temperature field in the section z=0.75 for A=0.25 (bridge heated from above, m=3, Ma= 3.75 10^4)

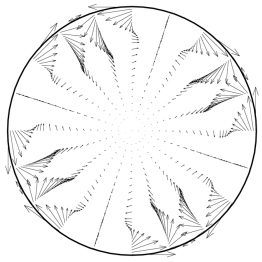

(c)

Velocity field in the section z=0.5 for A=0.2 (bridge heated from above, m=4, Ma= 3.95 10^4)

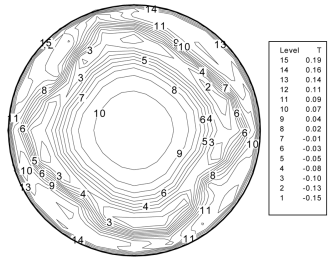

(f)

Temperature field in the section z=0.75 for A=0.2 (bridge heated from above, m=4, Ma= 3.95 10^4)

Figure 3.

Table III. Numerical and experimental results (bridge heated from above)

A	Ra	Ma	m (num.)	$f \cdot 10^{-2}$ (num.)	$Vp \cdot 10^{-2}$ (num.)	m (exp.)	$f \cdot 10^{-2}$ (exp.)	$Vp \cdot 10^{-2}$ (exp.)
0.25	$-7.2\ 10^3$	$3.75\ 10^4$	3	8.72	9.13	3	8.85	9.26
0.4	$-1.67\ 10^4$	$3.6\ 10^4$	2	3.40	5.34	2	5.4	8.4
0.5	$-2.52\ 10^4$	$3.5\ 10^4$	2	2.81	4.41	2	4.1	6.4

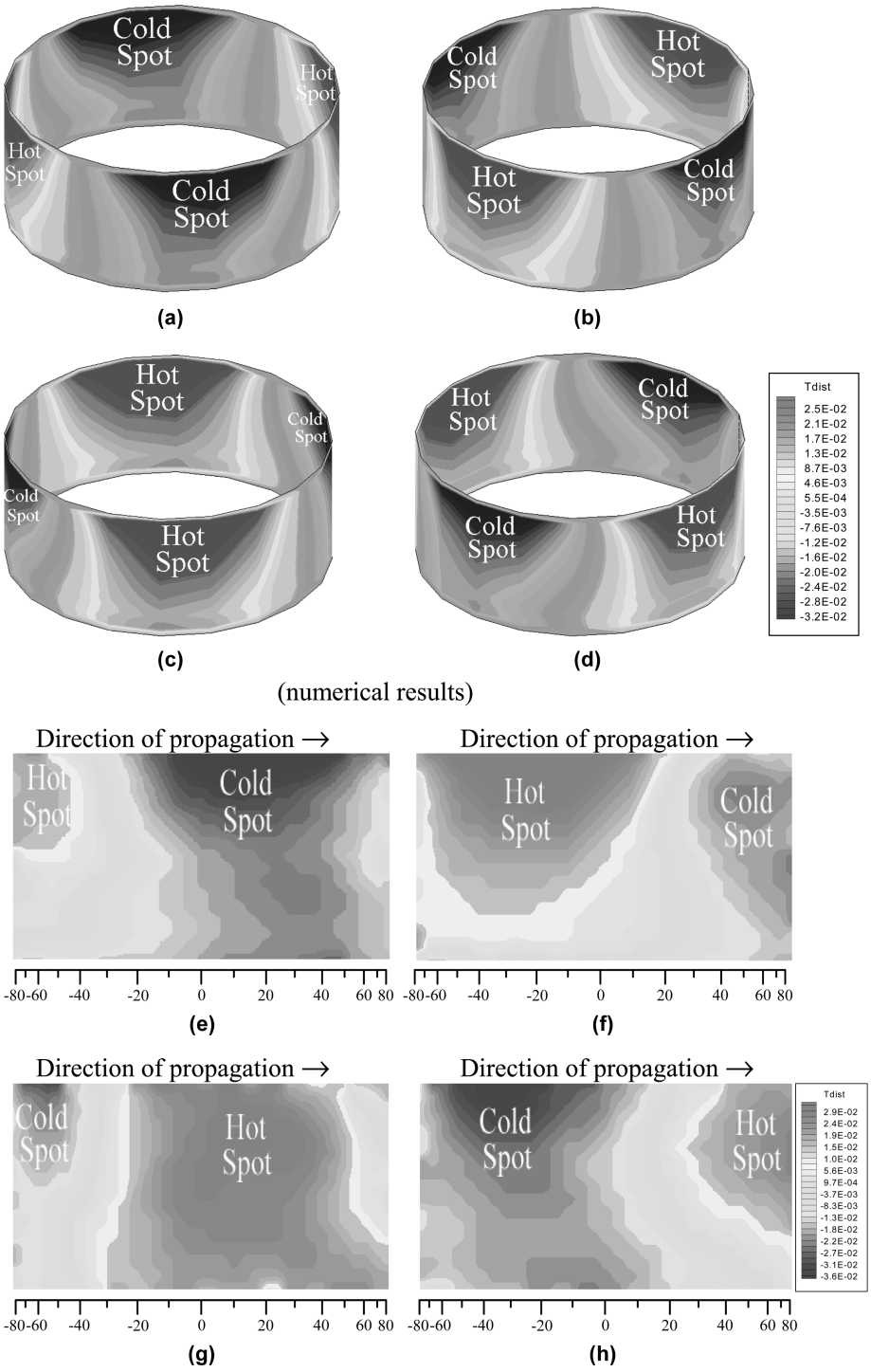

Figure 4.
Temperature disturbance on the bridge surface for A = 0.4 and travelling wave regime (Ma = 3.6 10^4 bridge heated from above, numerical and experimental results; the field is shown in a,b,c,d and e,f,g,h, corresponding respectively to t = 0, $\tau/4$, $\tau/2$, $3\tau/4$)

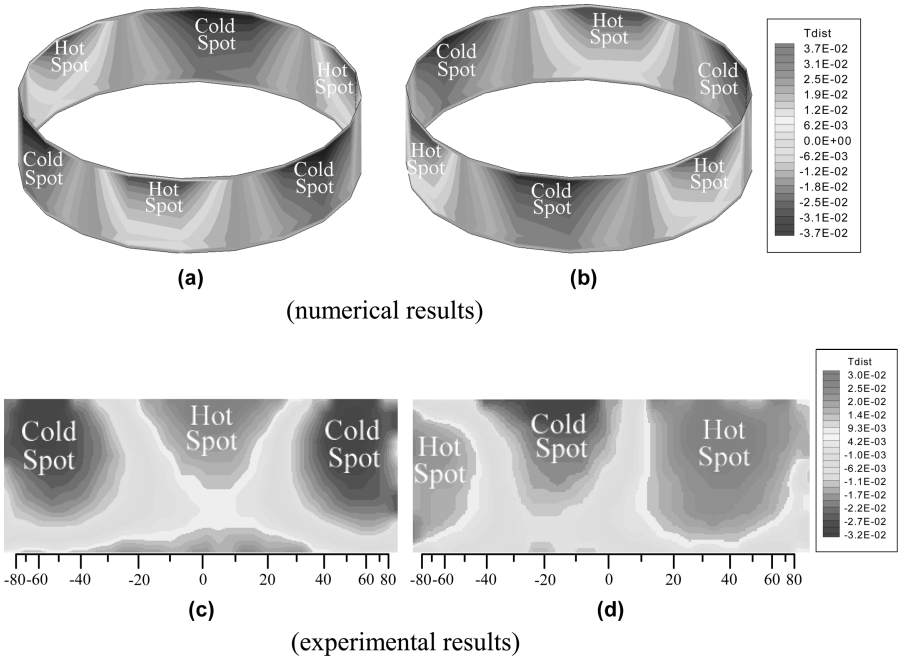

Figure 5.
Temperature disturbance on the bridge surface for A = 0.25 and standing wave regime (Ma = 3.75 10^4 bridge heated from above, numerical and experimental results; the field is shown in a,b and c,d corresponding respectively to t = 0, and t = τ/2)

t = 0, and t = τ/2) in perfect agreement with the numerical computed azimuthal wave numbers. Also the experimental frequencies are in agreement with the numerical computed ones and show a strong increase when the geometrical aspect ratio of the bridge is decreased (Table III).

The numerical results point out, moreover, that when heating from above the azimuthal critical wave numbers are almost the same with respect to the g = 0 situation (there is a difference only for the case A = 0.3 since m = 2 for μg conditions and m = 3 for 1g conditions). This result suggests utilizing liquid bridges heated from above during on the ground experiments dedicated to the definition of the experimental set-up (number of temperature sensors, thermographic visualization system, etc.) of microgravity experiments (since the flow patterns exhibit similar qualitative behaviours).

However, the results reveal that there is a certain increase in the critical Marangoni number and in the critical oscillation frequencies under the action of gravity with respect to the g = 0 condition (see Table II showing the non-dimensional frequency defined as $f = fcD^2/\alpha$ where fc is the computed critical frequency).

Gravity also produces variations in the frequency spectra. For heating from above, the structure of the oscillations becomes more complicated (Figure 6) and the oscillatory functions result from the superposition of a second function (with frequency f_1) on the basic fundamental frequency (f_0). Pure Marangoni convection periodic regimes characterized by the existence of a single

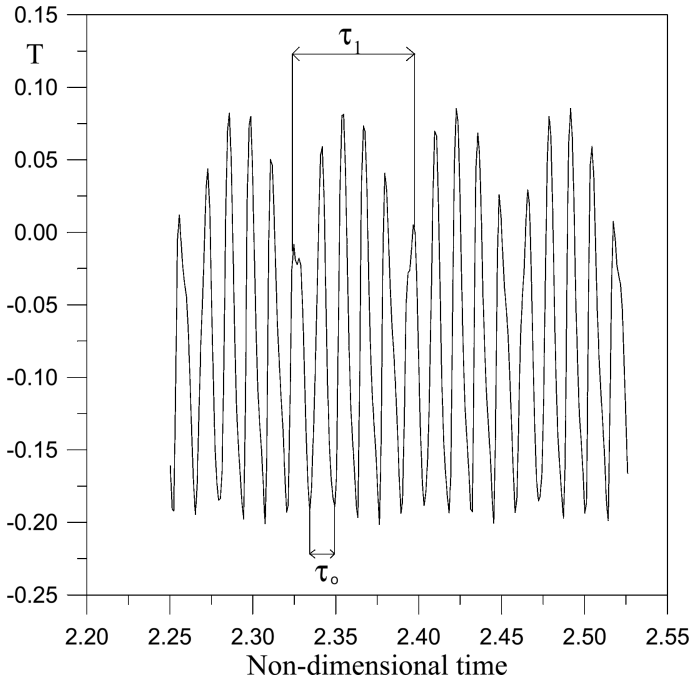

Figure 6.
Temperature oscillations in the point z = 0.75, r = 0.5, ϕ = 0, A = 0.5, Ma = 3.5 10^4, bridge heated from above

fundamental frequency turn in quasi-periodic regimes characterized by the superposition of uncommensurable frequencies when gravity effects with heating from above are considered.

The numerical results presented in this paper show, moreover, that, for all the aspect ratios considered when heating from above, the flow, immediately after the onset, may be properly described by the dynamic model of an "azimuthally standing wave".

The three-dimensional temperature disturbance consists in fact of a number m of a couple of spots (hot and cold) "pulsating" at the same azimuthal positions along the interface (minimum and maximum disturbances at fixed azimuthal positions). However, after a certain time, a travelling wave appears characterized by rotating temperature spots along the free surface of the liquid bridge.

This particular behaviour (an azimuthally standing wave that bifurcates in an azimuthally travelling wave after a certain time) is present for all the aspect ratios considered, but from the numerical calculations it can be deduced that the standing wave model is more stable for small aspect ratios (for $0.2 < A < 0.3$ the standing wave regime lasts for a long time) and less stable for high aspect ratios $A > 0.3$ (the pulsating regime turns in the rotatory regime after a short transition).

Also these results are in agreement with the experimental ones. In fact for A = 0.25 a standing wave regime has been observed (see Figure 5 with the hot and cold spots pulsating at fixed azimuthal positions) during the duration of

the experiment (four minutes) whereas for A = 0.4 a travelling wave regime (see Figure 4 with the hot and cold spots rotating in azimuthal direction) has been observed.

The stabilization of the standing wave regimes for low values of the aspect ratio is probably due to the fact that disturbances with higher mode number (low aspect ratio) propagate faster than those with smaller m (high aspect ratio) and hence have less time to interact and grow and determine the transition from the pulsating regime to the rotating one.

The propagation speed of the disturbances (see Chun and West, 1979) is defined as

$$\tilde{V}_P = \frac{2\pi R}{m\tau} \tag{5}$$

where R is the radius of the bridge, m the critical mode number and τ the period of the oscillations.

This velocity in non-dimensional form (see Table II) reads:

$$V_P = \tilde{V}_P \frac{D}{\alpha} = \frac{2\pi R}{m\tau^* D^2/\alpha} \frac{D}{\alpha} = \frac{\pi}{m} f \tag{6}$$

where τ* and f are the dimensionless period and the dimensionless frequency of the oscillations respectively.

Table II shows the computed values of Vp; the increase of the propagation speed of the disturbances takes place mainly for 0.3 < A < 0.4 and the numerical and experimental results presented in this paper show that the standing wave regime quickly develops into a travelling one if the aspect ratio is larger than 0.3.

A possible approach to give a final answer should consist of non-linear stability analyses for the solution of the non-linear disturbance amplitude equations after the onset of instability, to study the evolution of the system long after the onset of the instability.

5.2 Bridge heated from below

Figure 7 shows the situation of stationary Marangoni flow ($Ma < Ma_c$), in order to study the effect of aiding buoyancy forces on Marangoni convection.

When the bridge is heated from below and cooled from above, Marangoni and buoyancy flow act in the same direction. The velocity on the free surface increases with respect to heating from above (see the stream-function ψ in Figures 2c-d and 7a-b) and for A < 0.3 other counter-rotating vortex cells induced by buoyancy appear in the interior of the bridge. These additional vortex cells are called "Rayleigh-Benard" convection rolls. The critical Rayleigh number for the occurrence of these phenomena is 1,700 (as obtained experimentally by Schwabe *et al.* (1996)) and the Rayleigh numbers corresponding to the conditions considered in the present paper are larger than this value.

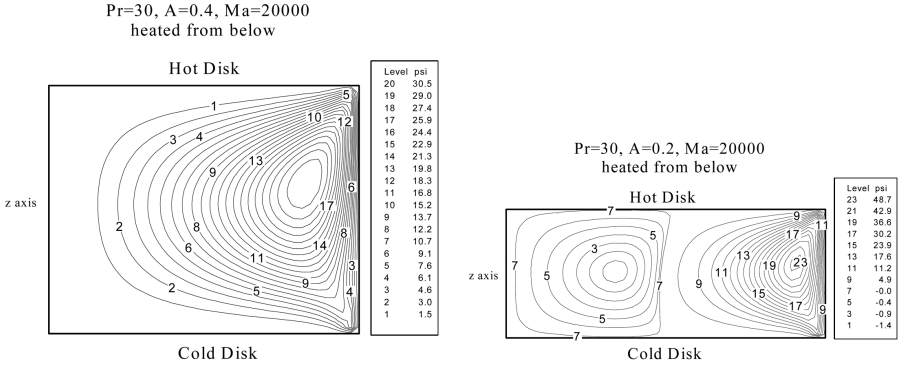

Streamlines in the generic meridian plane of the liquid bridge ($g=g_o$ bridge heated from below)

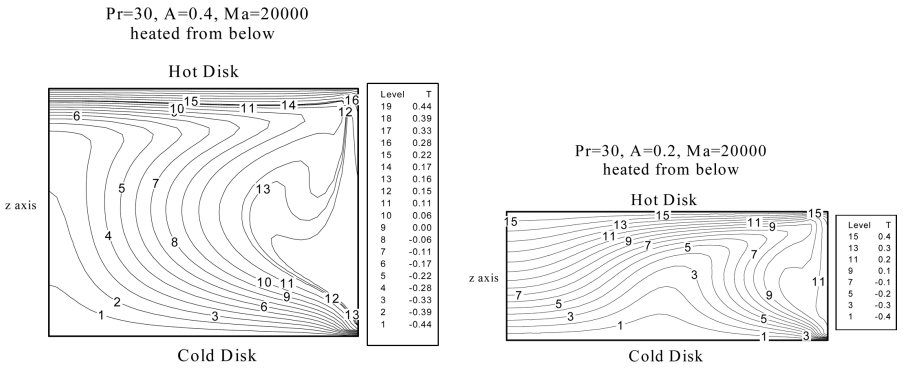

Temperature field in the generic meridian plane of the liquid bridge ($g=g_o$ bridge heated from below)

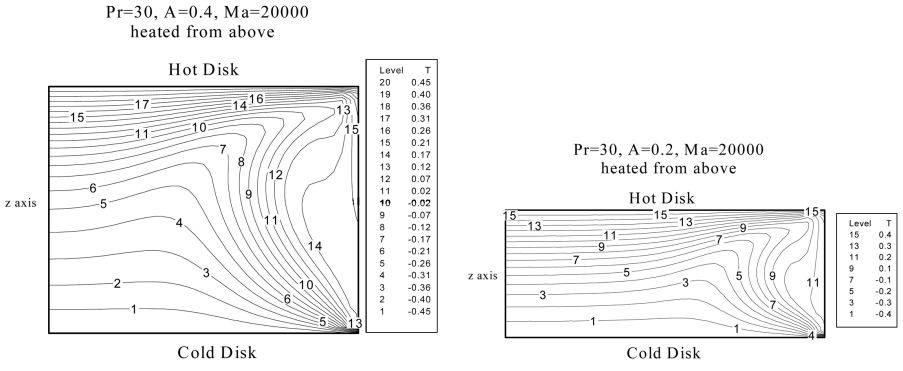

Temperature field in the generic meridian plane of the liquid bridge ($g=g_o$ bridge heated from above)

Figure 7.

Owing to the increase of the surface velocity (and of the return flow) and due to the presence of other buoyancy vortex cells in the inner part of the liquid bridge, the temperature field is strongly deformed (see Figure 7c-f) with respect to the case of heating from above (this behaviour is particularly evident for $A \leq 0.3$).

Then the critical Marangoni number for each case considered has been computed and the related supercritical state analysed. The results show that the azimuthal flow organization arising at the onset of instability completely changes according to whether the bridge is heated from above or from below.

The critical Marangoni numbers are slightly increased (Table IV). The azimuthal wave numbers are slightly different compared with the situation of heating from above (see Figure 8). Different values of m were obtained in well defined ranges of the aspect ratio as for heating from above, but for heating from below the ranges corresponding to a fixed value of m are completely different. For instance, Tables II and IV show: $m = 4$ for $A = 0.2$, $m = 3$ for $A = 0.25$ and $m = 2$ for $0.5 < A < 0.3$ for heating from above; when heating from below, the wave number is instead $m = 1$ for $A > 0.3$ (Figure 8a), $m = 2$ for $A = 0.25$ (Figure 8b) and $A = 0.3$, and $m = 3$ for $A = 0.2$ (Figure 8c).

Table V shows the numerical and experimental results related to values of the Marangoni number corresponding to typical supercritical conditions ($Ma \cong 1.5\ Ma_c$) in the case of the bridge heated from below. The dependence law between the critical azimuthal wave number and the geometrical aspect ratio provided by the numerical results is confirmed by the experimental results obtained using the microscale apparatus.

Looking at the temperature spots on the liquid bridge surface provided by the thermocamera in Figure 9e-h for $A = 0.4$ (in Figure 9 the period τ has been divided into four parts and the velocity field is shown in Figure 9a,b,c,d and e,f,g,h corresponding respectively to $t = 0$, $\tau/4$, $\tau/2$, $3\tau/4$ for experimental and numerical results) it is clear that the critical wave number is $m = 1$ since each spot has an angular extension corresponding to 180 degrees, whereas for $A = 0.25$ (Figure 10c-d) the critical wave number is $m = 2$ since each spot has an angular extension of 90 degrees.

These experimental results confirm that the azimuthal wave number is shifted to lower values with respect to the situation of heating from above. Moreover, looking at the numerical Figure 10a-b and the experimental Figure

Table IV.
Influence of the aspect ratio on the critical parameters (numerical results, bridge heated from below)

A	Ra	Ma_c	m	$f \cdot 10^{-2}$	$Vp \cdot 10^{-2}$
0.2	$3.8\ 10^3$	$3.3\ 10^4$	3	12.3	12.87
0.25	$5.4\ 10^3$	$3.0\ 10^4$	2	7.03	11.04
0.3	$7.23\ 10^3$	$2.8\ 10^4$	2	5.38	8.45
0.4	$1.18\ 10^4$	$2.55\ 10^4$	1	2.86	8.98
0.5	$1.73\ 10^4$	$2.4\ 10^4$	1	2.15	6.76

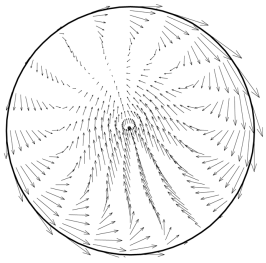

(a)

Velocity field in the section z=0.5 for A=0.5 (bridge heated from below, m=1, Ma= 4.2 10^4)

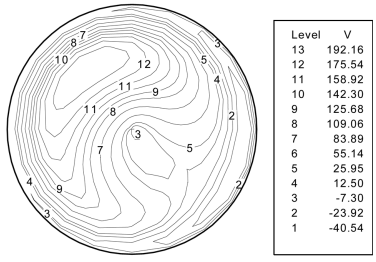

(d)

Radial velocity in the section z=0.75 for A=0.5 (bridge heated from below, m=1, Ma=4.2 10^4)

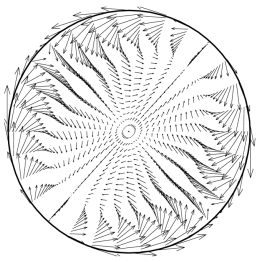

(b)

Velocity field in the section z=0.5 for A=0.25 (bridge heated from below, m=2, Ma= 4.2 10_4)

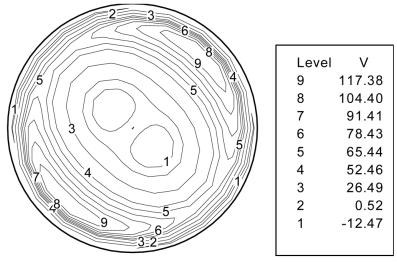

(e)

Radial velocity in the section z=0.75 for A=0.25 (bridge heated from below, m=2, Ma= 4.2 10_4)

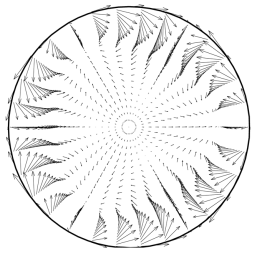

(c)

Velocity field in the section z=0.5 for A=0.2 (bridge heated from below, m=3, Ma= 4.4 10_4)

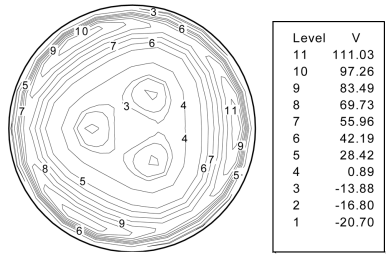

(f)

Radial velocity in the section z=0.75 for A=0.2 (bridge heated from below, m=3, Ma= 4.4 10_4)

Figure 8.

A	Ra	Ma	m (num.)	$f \cdot 10^{-2}$ (num.)	$Vp \cdot 10^{-2}$ (num.)	m (exp.)	$f \cdot 10^{-2}$ (exp.)	$Vp \cdot 10^{-2}$ (exp.)
0.25	$7.65\ 10^3$	$4.2\ 10^4$	2	7.35	11.54	2	8.6	13.5
0.4	$2.03\ 10^4$	$4.3\ 10^4$	1	3.19	10	1	4.9	15.3
0.5	$3.1\ 10^4$	$4.2\ 10^4$	1	2.50	7.85	1	3.4	10.6

Table V.
Numerical and experimental results (bridge heated from below)

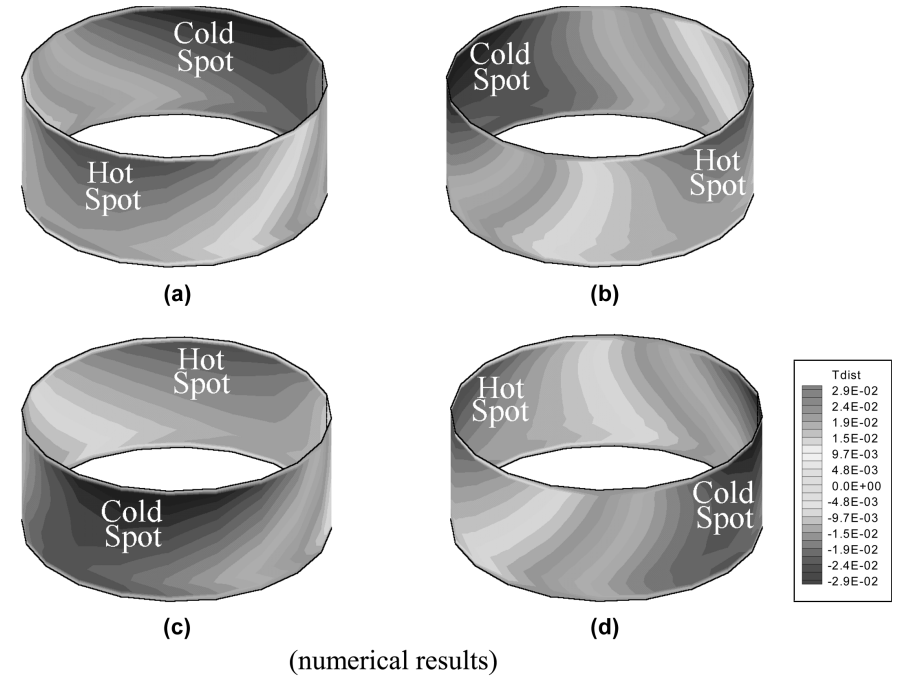

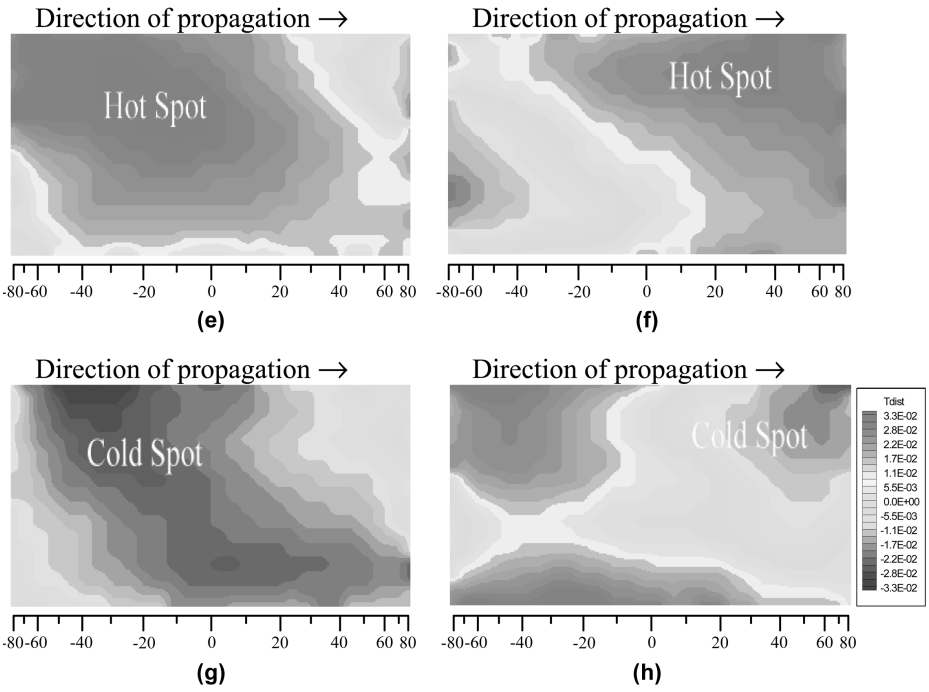

Figure 9.
Temperature disturbances on the bridge surface for A = 0.4 and travelling wave regime (Ma = 4.3 10^4 bridge heated from below, numerical and experimental results; the field is shown in a,b,c,d and e,f,g,h corresponding respectively to t = 0, $\tau/4$, $\tau/2$, $3\tau/4$)

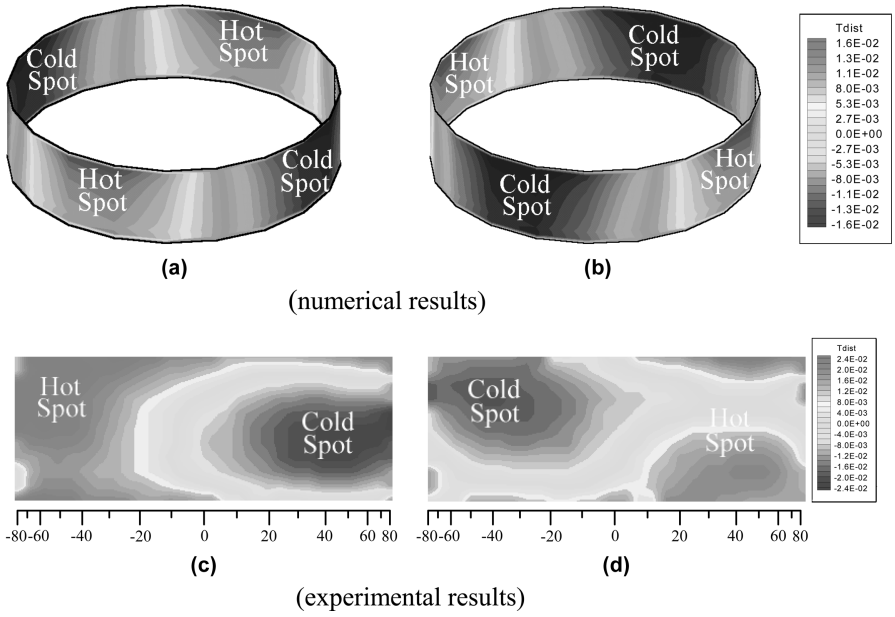

Figure 10. Temperature disturbances on the liquid bridge surface for A=0.25 and standing wave regime (Ma = 4.2 10^4 bridge heated from below, numerical and experimental results, the field is shown in a,b and c,d corresponding respectively to t = 0, and t = τ/2)

10c-d for A = 0.25 it is clear that the instability is established as a standing wave regime while Figure 9a-d (numerical) and Figure 9e-h (experimental) clearly show that for A = 0.4 a travelling wave regime is preferred.

For instance, Figure 12 shows the temperature oscillations measured by four "numerical probes" positioned at the same axial and radial coordinates but at different azimuthal positions in the case A = 0.5 (the sketch of the four thermocouples is shown in Figure 11).

When the bridge is heated from below the phase shift between the temperature profiles is $\pi/2$ when the two thermocouples are at 90 degrees (Figure 12a) and π when the two thermocouples are at 180 degrees (Figure 12b). When the bridge is heated from above the phase shift is π when the two considered thermocouples have an azimuthal shift of 90 degrees (Figure 12c) and there is no phase shift when the thermocouples are at 180 degrees (Figure

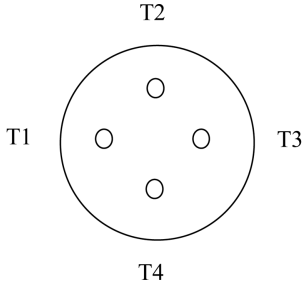

Figure 11. Sketch of the four numerical probes

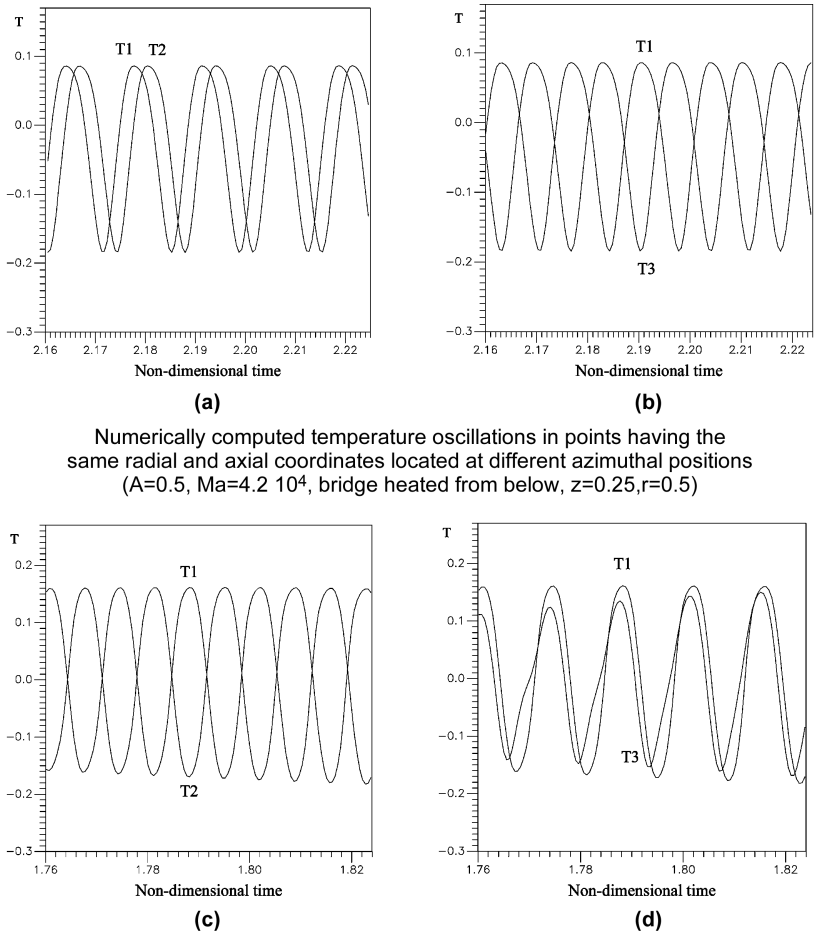

Figure 12.

12d). This behaviour can be explained considering that when the bridge is heated from above the critical azimuthal wave number is m = 2, whereas, when the direction of the gravity vector is reversed, the critical wave number is m = 1.

Regardless of the direction of the gravity vector (parallel or antiparallel to the axis) there is an increase of the mode number m with decreasing of the zone length (decreasing A), but the numerical results show that for heating from above the product 2mA is 1.7 while reversing the direction of the gravity 2mA is 1.1 (the constant values that appear in these laws have been computed as average values of the product 2mA over the range of aspect ratio investigated $0.2 \leq A \leq 0.5$; the value constant = 1.7 is characterized by a maximum uncertainty of 12 per cent with respect to the minimum or maximum value of 2mA, whereas in the case of heating from below the uncertainty is 18 per cent).

When heating from below the critical oscillation frequencies of the thermofluid-dynamic field always lie below the corresponding values for heating from above (Tables II and IV). This behaviour is confirmed by the present experimental results that show a decrease of the critical frequency for heating the bridge from below with respect to the heating from above condition.

This finding is in agreement with the experimental results obtained by Velten *et al.* (1991) in the case Pr = 49 and in contrast with those obtained by the same authors for Pr = 7 and Pr = 1 (since in these cases they observed that the critical oscillation frequencies for heating from above lie below the corresponding values for heating from below). Thus from the present results (obtained for Pr = 30) and those obtained by Velten *et al.* (1991) (for Pr = 1, 7 and 49) it can be argued that the Prandtl number Pr* corresponding to the "inversion" of the behaviour described above is in the range $7 < Pr^* < 30$.

The present numerical results point out, moreover, that the frequency spectrum is characterized by the existence of a single fundamental frequency and the behaviour of the oscillations is very regular compared with the heating from above situation .

Also this result is in agreement with the findings of Velten *et al.* (1991) in the case Pr = 49. In $C_{24}H_{50}$ zones in fact they did not find transition to aperiodic states in the whole range of aspect ratios and Marangoni numbers which was investigated.

The present numerical and experimental results reveal that, although the azimuthal structures emerging after the instability are different, the instability mechanism when the combined Marangoni-buoyant flow is considered is still of a hydrothermal type (i.e. it is related to the mechanism of hydrothermal waves propagation discussed by Kuhlmann and Rath (1993)) regardless of whether buoyancy effects are aiding or opposing Marangoni flow depending on the relative orientation of the gravity vector and of the temperature gradient. However, the standing wave regime is more stable for heating from below with respect to heating from above. On the basis of the interpretation given in section 5.1, this is probably due to the fact that disturbances travel faster when the bridge is heated from below as shown in Table IV.

The velocity of propagation of the disturbances is proportional to the ratio of the frequency of the temperature oscillations and of the azimuthal wave number. When the bridge is heated from below, the critical frequency decreases with respect to heating from above as discussed before; however, Vp increases due to the fact that the critical wave number is shifted to lower values (the decrease of m prevails with the decrease of the critical frequency). The increase of Vp gives rise to a stabilization of the pulsating regimes with respect to the condition of heating from above.

5.3 Discussion and comparison with other available results

Hirata *et al.* (1997a,b) compared mixed Marangoni-buoyant convection (for bridge heated from above) with the pure thermocapillary flow studying a

silicone oil liquid bridge (Pr = 30 and D = 5mm) under 1g and μg. They compared directly experiments performed in 1g and μg using a drop shaft tower without changing the experimental set-up (the onset of temperature oscillations was observed under μg while a capsule was free-falling and under normal gravity conditions when the capsule was kept at rest).

The critical temperature difference at which the steady state becomes unstable and undergoes a transition to an oscillatory state appeared to be smaller under μg conditions than that under 1g. Moreover, the fundamental frequency of the temperature oscillations was smaller under μg conditions compared to that under 1g conditions. The authors observed in many situations a quasi-periodic state with two fundamental frequencies under 1g conditions and a periodic state with only one fundamental frequency under μg conditions.

These results are in agreement with the numerical computations reported in this paper. Unfortunately, we cannot perform a quantitative comparison because the liquid bridges investigated by Hirata *et al.* (1997a,b) have a particularly deformed surface shape due to a non-cylindrical volume ($V \neq \pi R^2 L$).

To investigate the influence of buoyancy forces on the stability Velten *et al.* (1991) studied liquid zones heated from above and from below. For relatively large Prandtl number liquids (Pr = 1, 7, 49) they found that heating from below increases the critical Marangoni number compared to heating from above.

According to the present results, their experimental measurements revealed an intriguing behaviour concerning the different influences of buoyancy effects on the critical Marangoni numbers, in liquid bridges heated from below and from above.

The results reported in Figure 2 could give a simple explanation for the finding of Hirata *et al.* (1997a,b); in fact, buoyant forces stabilize stationary Marangoni convection in the zone heated from above because thermocapillary forces drive a surface flow of hot, lighter fluid downward against buoyancy.

If this were correct, one should expect, in zones heated from below under normal gravity, larger surface flow velocities and correspondingly smaller Ma_c compared to zones heated from above. On the contrary, the critical Marangoni numbers measured experimentally (Velten *et al.*, 1991) and predicted numerically in this paper are always larger for bridges heated from below than those found for heating from above. This demonstrates that buoyancy stabilizes stationary Marangoni convection not only when thermocapillary and buoyant forces are counteracting but also when these mechanisms are concurrent. A possible explanation for this result is that the onset of the Marangoni instability is related not only to the magnitude of the velocities (because this instability is not caused by inertial effects but it is hydrothermal in nature) but should be explained considering the combined effect of the velocity and temperature fields.

It is a well-known fact that in the oscillatory regime the time dependence of the Marangoni flow is characterized by small accelerations and decelerations of the primary toroidal convection roll which are caused by minute variations of

the surface temperature distribution. The main reason for the instability is the existence of a "cold radially elongated zone" near the hot disk, which is created by the return flow that brings cool fluid away from the cold wall along the symmetry axis. The cold liquid is carried towards the hot surface at a rather high position. This cold zone can generate cold temperature disturbances from inside near the hot free surface and these disturbances can influence the surface temperature distribution giving rise to the instability. In previous results it was pointed out that the instability of Marangoni flow is related to the convective radial heat transport coupled with Marangoni effect (Wanschura *et al.*, 1995). The mechanism of oscillations is based on the temporal interaction between the temperature distribution within the flow field (in particular the "cold radially elongated zone" established inside the liquid bridge near the hot disk as pointed out by Shevtsova and Legros (1997)) and the temperature sensitive free surface (this is the reason the surface temperature spots always appear near the hot disk). The transition from steady to oscillatory regime occurs when the cold radially elongated zone is able to influence the thermocapillary surface (the sensitivity of the free surface plays a "critical role" in the instability mechanism).

In this paper it has been shown that heating from above results in lower radial temperature gradients near the hot disk with respect to the case of zero-g conditions whereas heating from below results in larger surface velocities (with respect to the case of heating from above).

In the first case the weak stabilization of the flow with respect to the situation of zero-g conditions can be explained by the reduced sensitivity of the free surface with respect to the case of zero-g conditions; in this case, in fact, the temperature of the cold radially elongated zone is weakened by the buoyancy effects, which slow down the fluid near the cool disk carried in the return flow.

In the latter case (heating from below) the strong stabilization of the flow with respect to the situation of heating from above is due to the fact that small surface temperature disturbances induced near the hot disk from inside by the cold radially elongated zone have a weaker impact on the acceleration or deceleration of the main surface flow (the sensitivity of the free surface is decreased by the strong surface velocities).

The influence of the buoyancy forces on the radial temperature gradients inside the bridge and on the magnitude of the surface velocity can therefore explain the weak stabilization that occurs when the bridge is heated from above with respect to the situation of zero-g conditions and the strong stabilization that occurs when the bridge is heated from below with respect to the situation of heating from above.

The results of the linear stability analyses of Kuhlmann *et al.* (1996) and Wanschura *et al.* (1997) explain this behaviour in terms of a delicate balance between stabilizing and destabilizing buoyancy effects.

They suppose that, since hydrothermal waves are characterized by strong axial vorticity while buoyant convection favours convection rolls with strong horizontal vorticity, therefore both types of convection structures are

incompatible in the sense that their respective transport mechanisms exclude each other, yielding a stabilization of the basic state. Regarding the occurrence of the standing wave regime or of the travelling wave regime, unfortunately the linear stability analyses cannot provide information on this subject since they do not consider the spatio-temporal behaviour of the system.

The only experimental information available is that of Velten *et al.* (1991), that reported in the excellent overview of Frank and Schwabe (1998) and that of Shevtsova *et al.* (1998).

For both heating conditions, several aspect ratios and different Prandtl numbers, Frank and Schwabe (1998) describe in detail the structure of pulsating and rotating regimes for the first time through direct observation of the azimuthal flow structure. Comparing the results from three different Prandtl numbers (Pr = 1,7,49) and comparing heating from above with heating from below, Velten *et al.* (1991) pointed out that the occurrence of rotating regimes is largely decreased into the latter case.

This behaviour can be explained on the basis of the present results. For heating from below the rotating regimes do not disappear; they are simply postponed in time due to the fact that the pulsating regimes are more stable and take a long time to develop into rotating ones.

Velten *et al.* (1991) explain the fact that pulsating regimes (which they call m = 0 axially running waves with deformed wave front) are favoured for heating from below on the basis of the theory of Xu and Davis (1984). According to this theory, the energy source for the axially running waves and for the travelling waves should be the radial temperature gradient and the radial velocity gradient respectively. Velten *et al.* (1991) attribute the decrease of the observed rotating regimes in the case of heating from below to the reduction of the radial velocity gradient and to the increase of the radial temperature gradient due to the buoyancy effects.

This theory, however, cannot be accepted on the basis of the present results. The pulsating regime in fact is not a "pure" axially running wave with m = 0 and, therefore, it does not correspond to the prediction of Xu and Davis (1984) obtained in the case of infinite liquid bridges.

Regarding the transition between the pulsating regime and the travelling regime that has been observed in the present results for all the aspect ratios considered, very little information is available in the literature. Velten *et al.* (1991) in many cases found unexpected behaviours (that they were not able to explain) that could be interpreted as transition between pulsating and rotating regimes.

Using three thermocouples having the same axial and radial coordinates but different azimuthal positions, they measured in many situations phase shifts changing continuously in time.

When the regime is pulsating (surface temperature spots pulsating at fixed azimuthal positions) and two thermocouples are located on the same spot, they give temperature signals that do not show phase difference; when the regime becomes rotating the two thermocouples give signals that show a constant

phase shift related to the angular distance between them. Between these two regimes a hybrid regime exists that should be called "pulso-rotating"; during this regime the phase shift between the two thermocouples increases in time starting from zero until it reaches a constant value corresponding to the rotating regime; during this phase the phase shift corresponds to values of the azimuthal wave number that are not entire, as observed by Velten *et al.* (1991).

However, transition from a standing wave regime to travelling wave regime has been observed directly by Monti *et al.* (1998) in the case of a liquid bridge of silicone oil (Pr = 45) and aspect ratio A = 0.7 (m = 1), and by Shevtsova *et al.* (1998) in the case of Pr = 105 and A = 0.6 (m = 1). These authors used four thermocouples located at the same axial and radial coordinates but at different azimuthal positions to "detect" the transition from the pulsating regime to the rotating one.

6. Conclusions

The interaction of buoyancy and Marangoni flow in a vertical cylindrical liquid bridge with an adiabatic free lateral surface and isothermal top and bottom walls has been studied numerically in a transient three-dimensional simulation and experimentally using a microscale facility.

Most of the existing information in the literature for high Prandtl numbers ($O(10\text{-}10^2)$) comes from experiments and from linear stability analysis based on a linearized form of the equations that does not permit any information to be obtained on the spatio-temporal behaviour of the liquid bridge in the supercritical state. In the present paper a systematic and parametric analysis of the features of the mixed buoyancy-Marangoni instability for a high Prandtl liquid (Pr = 30) is performed through full 3D solution of the time-dependent, non-linear and complete Navier Stokes equations.

The spatio-temporal behaviour of the supercritical regime has been studied in detail (no numerical works are available in the literature on this subject and linear stability analyses are unable to do this).

The influence of buoyancy effects on the flow instability and in particular on the critical wave number (m) and on the spatio-temporal structures (pulsating or rotating) has been considered.

The results show that the azimuthal flow organization arising at the onset of instability completely changes according to whether the bridge is heated from above or from below. In particular, when the liquid bridge is heated from below, the critical Marangoni number is larger and the critical wave number (m that represents the number of sinusoidal distortions in azimuthal direction) is smaller compared with when the bridge is heated from above.

These results show that gravity effects may have a large effect on Marangoni flow instability when the bridge is heated from below, even if the experiments are performed reducing the typical length of the liquid bridge to a few millimetres (microscale experimentation).

For the dimensionless wave number of the instability two correlation functions are found: 2mA = 1.7 when heating from above and 2mA = 1.1 when heating from below.

For the first time the influence of the gravity field on the transition from standing wave regimes to travelling wave regimes has been studied. The results indicate that the mechanism of the instability is of a hydrothermal type and characterized by a transition from a pulsating regime to a rotating regime. This mechanism is present for both heating conditions, but for heating from below the standing wave regime is more stable.

The weak stabilization that occurs when the bridge is heated from above with respect to the situation of zero-g conditions and the strong stabilization that occurs when the bridge is heated from below with respect to the situation of heating from above have been explained in terms of the influence of the buoyancy forces on the radial temperature gradients inside the bridge and on the magnitude of the surface velocity.

For the first time the influence of the gravity field on the Fourier spectra of the supercritical state has been examined using numerical simulation.

References

Chun, C.H. and West, W. (1979), "Experiments on the transition from the steady to the oscillatory Marangoni convection of a floating zone under reduced gravity effect", *Acta Astronautica*, Vol. 6, p. 1073.

Fletcher, C.A.J. (1991), *Computational Techniques for Fluid-Dynamics*, Springer Verlag, Berlin.

Frank, S. and Schwabe, D. (1998), "Temporal and spatial elements of thermocapillary convection in floating zones", *Experiments in Fluids*, Vol. 23, p. 234.

Hirata, A., Sakurai, M. and Ohishi, N. (1997a), "Effect of gravity on Marangoni convection in a liquid bridge", *J. Jpn. Soc. Microgravity Appl.*, Vol. 14, p. 130.

Hirata, A.A., Sakurai, M., Ohishi, N., Koyama, M., Morita, T. and Kawasaki, H. (1997b), "Transition process from laminar to oscillatory Marangoni convection in a liquid bridge under normal and micro gravity", *J. Jpn. Soc. Microgravity Appl.*, Vol. 14, p. 137.

Kuhlmann, H.C. and Rath, H.J. (1993), "Hydrodynamic instabilities in cylindrical thermocapillary liquid bridges", *J. Fluid Mech.*, Vol. 247, p. 247.

Kuhlmann, H.C., Wanschura, M., Leypoldt, J. and Rath, H.J. (1996), "Buoyant-thermocapillary convection and three-dimensional flow in liquid bridges: comparison of numerical and experimental results", *Microgravity Quarterly*, Vol. 6, p. 65.

Lappa, M. and Savino, R. (1999), "Parallel solution of three-dimensional Marangoni flow in liquid bridges", *Int. J. Num. Meth. Fluids*, Vol. 31, p. 911.

Monti, R. and Fortezza, R. (1986), "Non-intrusive techniques for thermal measurements in microgravity fluid science experiments", *Adv. Space Res.*, Vol. 6, p. 69.

Monti, R., Savino, R. and Lappa, M. (1997), "Oscillatory thermocapillary flows in simulated floating zones with time-dependent boundary conditions", *Acta Astronautica*, Vol. 41, p. 863.

Monti, R. *et al.* (1995), "First results from 'onset' experiment during Spacelab Mission D-2", in Sahm, P.R., Keller, M.H. and Schiewe, B. (Eds), *Proceedings of the Norderney Symposium on Scientific Results of the German Spacelab Mission D2*, p. 247.

Monti, R., Savino, R., Lappa, M. and Fortezza, R. (1998), "Scientific and technological aspects of a sounding rocket experiment on oscillatory Marangoni flow", *Space Forum*, Vol. 2, p. 293.

Muehlner, K.A., Schatz, M.F., Petrov, V., McCormick, W.D., Swift, J.B. and Swinney, H.L. (1997), "Observation of helical traveling-wave convection in a liquid bridge", *Phys. Fluids*, Vol. 9 No. 6, p. 1850.

Neitzel., G.P., Chang, K.T., Jancowski, D.F. and Mittelmann, H.D. (1992), "Linear stability of thermocapillary convection in a model of the float-zone crystal-growth process", *Phys. Fluids*, Vol. A5, p. 108.

Preisser, F., Schwabe, D. and Scharmann, A. (1983), "Steady and oscillatory thermo capillary convection in liquid columns with free cylindrical surface", *J. Fluid Mech.*, Vol. 126, p. 545.

Rupp, R., Muller, G. and Neumann, G. (1989), "Three-dimensional time dependent modelling of the Marangoni convection in zone melting configurations for GaAs", *Journal of Crystal Growth*, Vol. 97, p. 34.

Savino, R. and Monti, R. (1996), "Oscillatory Marangoni convection in cylindrical liquid bridges", *Phys. Fluids*, Vol. 8, p. 2906.

Schwabe, D., Hintz, P. and Frank, S. (1996), "New features of thermocapillary convection in floating zones revealed by tracer particle accumulation structures", *Microgravity Sci. Technol.*, Vol. 9, p. 163.

Schwabe, D., Scharmann, A.A., Preisser, F. and Oeder, R. (1978), "Experiments on surface tension driven flow in floating zone melting", *J. Crystal Growth*, Vol. 43, p. 305.

Shevtsova, V. and Legros, J.C. (1997), "Influence of the free surface shape on stability of liquid bridges", Joint Xth European and VIth Russian Symposium on Physical Sciences in Microgravity, St Petersburg, Russia, 15-21 June.

Shevtsova, V., Mojahed, M. and Legros, J.C. (1998), "The loss of stability in ground based experiments in liquid bridges", 49th Congress of the International Astronautical Federation, Melbourne, Australia, 28 September-2 October.

Velten, R., Schwabe, D. and Scharmann, A. (1991), "The periodic instability of thermocapillary convection in cylindrical liquid bridges", *Phys. Fluids A*, Vol. 3, p. 267.

Wanschura, M., Kuhlmann, H.C. and Rath, H.J. (1997), "Linear stability of two-dimensional combined buoyant-thermocapillary flow in cylindrical liquid bridges", *Physical Review E*, Vol. 55 No. 6, p. 7036.

Wanschura, M., Shevtsova, V., Kuhlmann, H.C. and Rath, H.J. (1995), "Convective instability mechanism in thermocapillary liquid bridges", *Phys. Fluids*, Vol. A5, p. 912.

Xu, J.J. and Davis, S.H. (1984), "Convective thermocapillary instabilities in liquid bridges", *Phys. Fluids*, Vol. 27, p. 1102.